Earthquake Geotechnical Engineering for Protection and Development of Environment and Constructions – Silvestri & Moraci (Eds)
© 2019 Associazione Geotecnica Italiana, Rome, Italy, ISBN 978-0-367-14328-2

Experimental study on seismic ground motion amplification pattern of soil-structure interaction system

Z.M. Zhang
Department of Geotechnical Engineering, Tongji University, Shanghai, China
Department of Civil, Architectural & Environmental Engineering, University of Naples Federico II, Naples, Italy

E. Bilotta
Department of Civil, Architectural & Environmental Engineering, University of Naples Federico II, Naples, Italy

Y. Yuan
State Key Laboratory of Disaster Reduction in Civil Engineering, Tongji University, Shanghai, China

H.L. Zhao
Department of Civil Engineering, Shanghai University, Shanghai, China

H.T. Yu
Key Laboratory of Geotechnical and Underground Engineering of Ministry of Education, Tongji University, Shanghai, China

ABSTRACT: A series of 1 g shaking table tests are performed to investigate the seismic ground motion amplification pattern, including free-field test and soil-structure test. This study outlines two issues. First, for the free-field model, the comparison of both transfer functions and natural frequencies between the experimental data and the analytical solutions was made. It is found that the measured transfer functions could reflect the characteristics of analytical solutions on the whole. Second, the influence of the existing of atrium-style subway station on acceleration responses of soil was emphasized. Two influencing factors were thought to have an important contribution to the seismic ground motion amplification pattern. One is the frequency content of input ground motion and the other is the height of the underground structure, which determined the relationship between seismic wavelength and the size of the structure. This paper only presents the acceleration responses, but the conclusion will also provide a possibility to explain other dynamic responses of soil-structure model. This study also provides preliminary criteria to determine whether the existing of an underground structure can be neglected in the design of a surface structure.

1 INTRODUCTION

In view of less and less above ground space for engineering construction, the population growth and transportation problems in urban areas, the use of underground structures like subways and tunnels are rapidly increasing in a lot of countries and populous cities (Alielahi et al., 2015). After the Hyogoken-Nambu earthquake of January 17, 1995 in Japan, which caused utter devastation of the Daikai subway station and severe damage to some other stations, seismic design and analysis of underground structures have attracted more and more attention than before.

The seismic ground response around underground structures will usually be different from that in free field, as shown in several studies (Besharat et al., 2014; Assimaki et al., 2005; Baziar et al., 2014; Tsinidis et al., 2014; Moghadam et al., 2016; Guan et al., 2016; Wang et al., 2018;

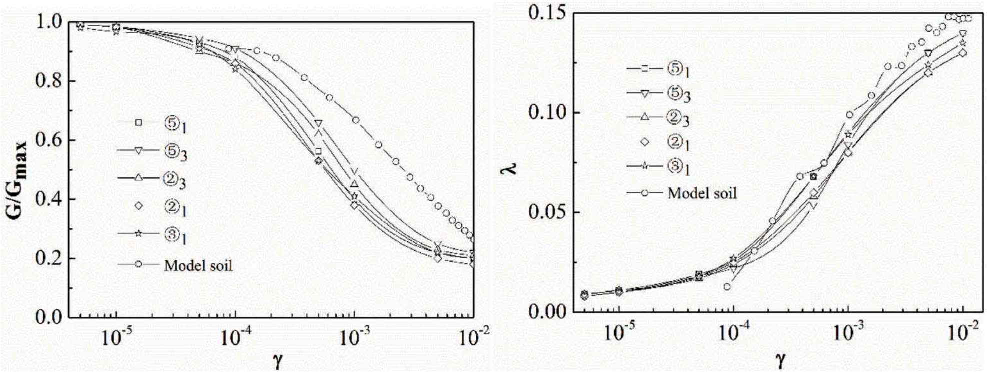

Figure 1. Normalized shear modulus curves and damping ratio curves of model soil and in situ soil.

Guo et al., 2013). However, it is worth mentioning that existing research mainly focuses on underground tunnels.

The studies of large-span underground structures with very shallow depth such as cut-and-cover subway station are very few and direct experimental evidence is still lacking (Hashash et al., 2018). In this work an atrium-style subway station is taken into account. A series of 1 g shaking table tests are designed and performed to investigate the seismic ground motion amplification pattern, including free-field test and soil-structure test. The similitude ratio of geometry was taken as 1/30. Galvanized steel wire and micro-concrete were used to simulate the prototype steel rebar and concrete, respectively. The mass ratio of micro-concrete was determined as cement:coarse sand:lime:water=1:5:0.64:1.18. The compressive yield strength and elastic modulus of such a micro-concrete were measured in uniaxial compression test as 10.68 MPa and 1.32×10^4 MPa, respectively. In order to satisfy the similitude ratio, the model soil was made of a mix of sand and sawdust with the optimal mass ratio of 1:2.5 (sawdust to sand). Figure 1 shows the G/Gmax vs. γ curve and λ vs. γ curve of both prototype and model soil, where G, Gmax, λ, γ are the shear modulus, the maximum shear modulus, the soil damping ratio and shear strain, respectively. A 48-m-thick prototype soil down from the surface is considered, with the buried depths of each layer's bottom (①$_1$, ②$_1$, ②$_3$, ③$_1$, ⑤$_1$, and ⑤$_3$, see DGJ08-37-2012, Code for investigation of geotechnical engineering) equal to 1.7 m, 3.2 m, 6 m, 17 m, 31 m, and 48 m, respectively. The other properties of model soil can be found in the reference (Bao et al., 2017). For the free-field model, a comparison between the test results and analytical solutions is made to prove the reliability of the model. Afterwards, the seismic ground responses of soil-structure model will be compared with those of free-field model, both on the ground surface and along the depth of ground. Based on the comparison, criteria will also be provided to determine whether the existing of an underground structure can be neglected in the design of a surface structure. In this paper, the discussion is restricted to the seismic ground responses of both the free-field model and the soil-structure interaction model. Figures 2 and 3 present the experimental procedure and the layout of accelerometers of the two models, respectively, for the sake of convenient discussion. Any other details of free-field test and soil-structure test can be found in previous work (Zhang et al., 2019).

2 VERIFICATION

Checking the dynamic characteristics of the ground is the most direct way to validate the reliability of the shaking table test. Resonance frequencies of model ground can be usually evaluated from the peak of transfer function in the frequency domain, which is calculated by dividing Fourier amplitude of the acceleration at the ground surface (recorded by A15 accelerometer) to the Fourier amplitude of the input acceleration (recorded by the shaking table itself). As a comparison, the analytical solutions of transfer function for the free-field model will also be presented here. For the uniform and damped soil on rigid rock, the transfer

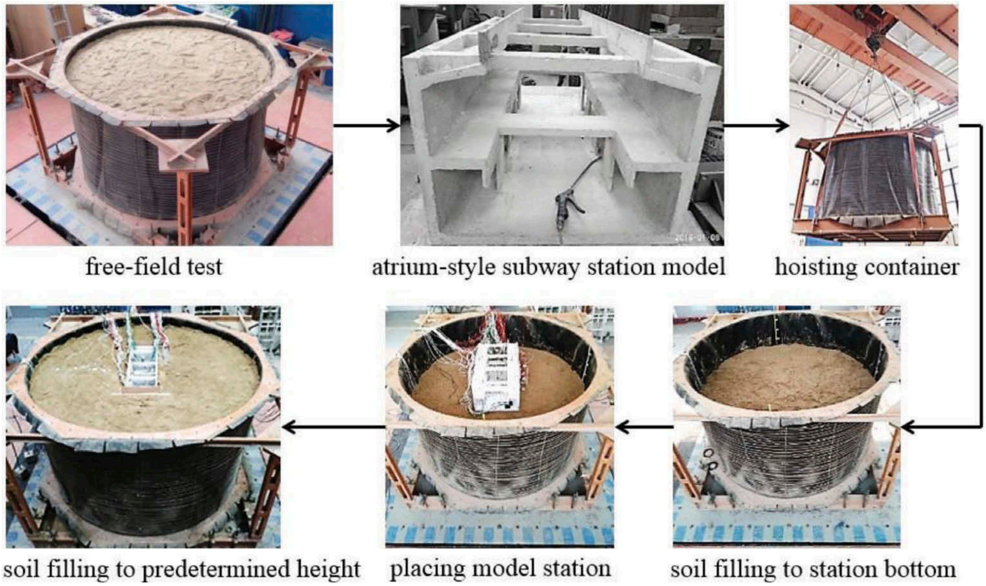

Figure 2. Photos of experimental procedure.

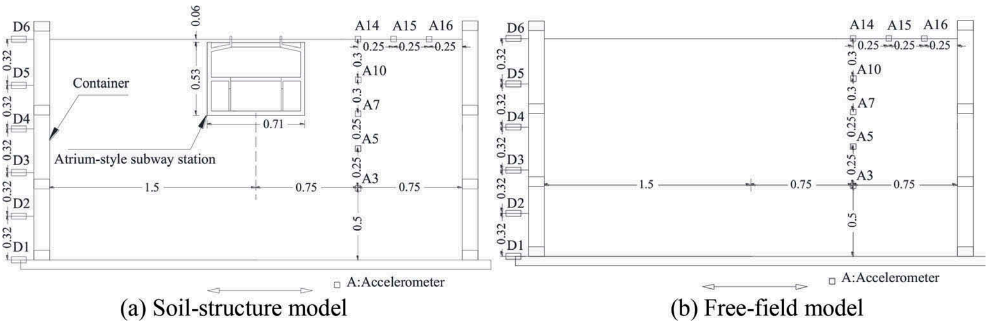

Figure 3. Layout of accelerometers of the two models (unit: m).

function $F(\omega)$ and n$^{\text{th}}$ natural frequency f_n can be determined from the following formula (Kramer, 1996):

$$|F(\omega)| \approx \frac{1}{\sqrt{\cos^2\left(\frac{\omega H}{v_s}\right) + \left[\xi\left(\frac{\omega H}{v_s}\right)\right]^2}} \tag{1}$$

$$f_n = \frac{(2n+1)v_s}{4H} \tag{2}$$

where ω is angular frequency ($\omega = 2\pi f$, f represents the discrete Fourier transform frequencies between 0 and 50 Hz for this test), H is soil thickness, v_s and ξ are shear wave velocity and damping ratio of the soil, respectively. The actual damping ratio of the soil in the test was determined by the "half-power bandwidth" calculation (Blackwell et al., 2007; Jiang et al., 2010). The half-power is calculated by measuring the bandwidth of the frequency curve down from the resonant peak. The damping ratio is then found using Eq. (3):

$$\xi = \frac{f_{n2} - f_{n1}}{2f_n} \tag{3}$$

where f_{n1} and f_{n2} ($f_{n1} < f_{n2}$) are half-power points at which the output power has dropped to 0.707 times of the peak value at frequency f_n. The measured curves of transfer function were not smooth due to noise interference. Interpolation and curve fitting were conducted on the measured curves. Finally, the calculated damping ratios for first, second and third modes are 6.18%, 8.82% and 8.35%, respectively. In view of the major contribution of mode 1 to the dynamic response, the damping ratio 6.18% is selected and substituted into Eq. (1). The measured transfer functions were obtained from the points A14-A16 at ground surface of free-field model. The comparison of analytical and measured transfer functions is presented in Figure 4. The comparison of analytical and measured first three natural frequencies is illustrated in Table 1. In addition to the ground surface, the comparison of analytical and measured transfer functions at different depths of ground is also shown in Figure 5.

It can be seen from Figures 4 and 5 that the measured transfer function on the ground surface could reflect the characteristics of analytical solutions on the whole, though some differences in amplitude. It is also found from Table 1 that the natural frequencies evaluated from surface transfer function were very similar to those estimated from the analytical solutions. The deviations were less than 4%. As far as the transfer function at different depths of ground are concerned (see Figures 4 and 5), the measured transfer function from the upper part of the ground layer (e.g. A14, A10, A7) were much closer to the analytical solutions than that from the lower part (e.g. A5, A3), especially with respect to the amplitude. This might be attributed to the fact that the damping adopted in analytical solutions was based only on the first mode and applied to the whole model, which might deviate from the actual situation. On the whole, the test results of free-field model had good agreement with analytical results.

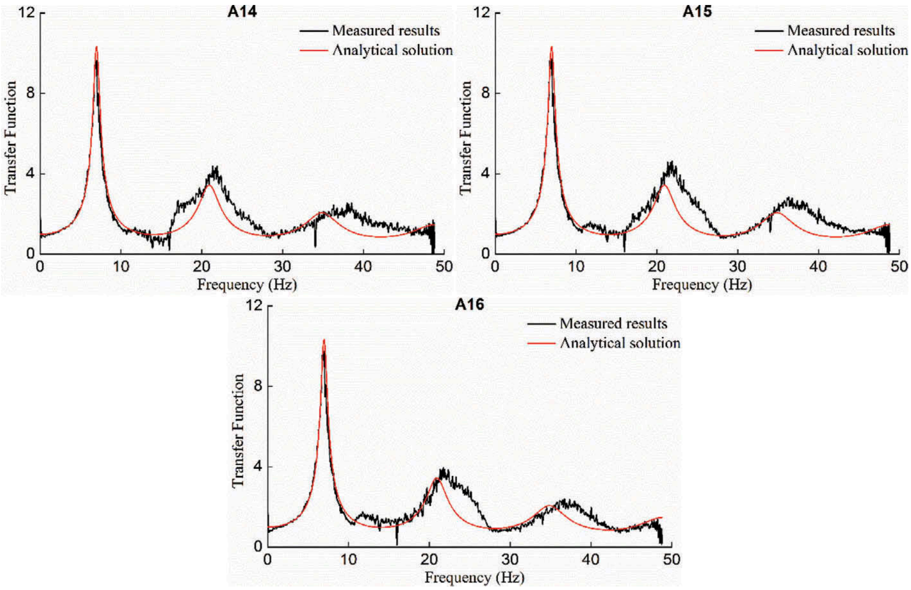

Figure 4. Comparison of analytical and measured transfer functions of surface ground.

Table 1. Comparison of analytical and measured first three natural frequencies.

Model	Natural frequency		
	1st	2nd	3rd
Analytical solution [Eq. (2)]	6.97	20.92	34.86
Test (case:WN1)	6.89 (-1.15%)	21.58 (+3.15%)	36.20 (+3.84%)

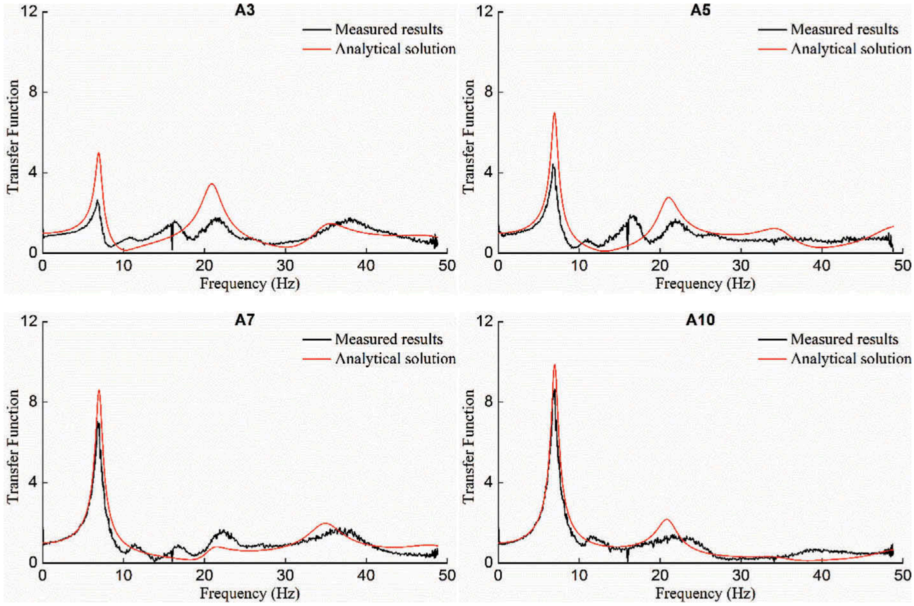

Figure 5. Comparison of analytical and measured transfer functions at different depths of ground.

3 TEST RESULTS

The acceleration was recorded at several locations in both horizontal and vertical directions during shaking. The presence of underground subway station in the soil could modify the wave propagation process. In this study, the seismic ground responses around the subway station will be discussed with respect to the horizontal component at ground surface and along depth. Since the accelerometers of the free-field model and the soil-structure model are arranged at same places in the soil, it will be easy to compare the results in the two tests. The test results under harmonic ground motions of 1~33 Hz are shown in the following.

3.1 *Influence of atrium-style subway station on acceleration responses of ground along depth*

Previous numerical study revealed that the tunnel did not affect the free field response at dimensionless period (the ratio of wavelength of incident wave and diameter of the tunnel or cavity) greater than 10 (Moghadam et al., 2016) or 8 (Alielahi et al., 2015). But until now, this finding has not been verified by any experimental studies. Moreover, whether this conclusion is true for other large-span underground structures such as cut-and-cover subway station with very shallow depth still remains unknown. Here the above finding can be verified as follows.

f, λ, H_s and V_s denote the frequency of input motion, wavelength, the height of subway station and shear velocity of model soil respectively. For this study, V_s=44.8m/s. Hence,

- when f=9 Hz, then $\lambda/8=V_s/(8\times f)=0.62$ m $>$ $H_s=0.6$ m;
- when f=15 Hz, then $\lambda/8=V_s/(8\times f)=0.37$ m $<$ $H_s=0.6$ m.

This reveals why the subway station almost had no impact on the ground when dimensionless period greater than 8, while bigger impact on the ground when dimensionless period lower than 8, as shown in Figure 6.

3.2 *Influence of atrium-style subway station on acceleration responses of ground surface*

The acceleration amplification frequency spectra for free-field model and soil-station model at different positions on ground surface are presented in Figure 7a and 7b, respectively. It can be seen from Figure 7a that for free-field model when the frequencies of input motion were lower

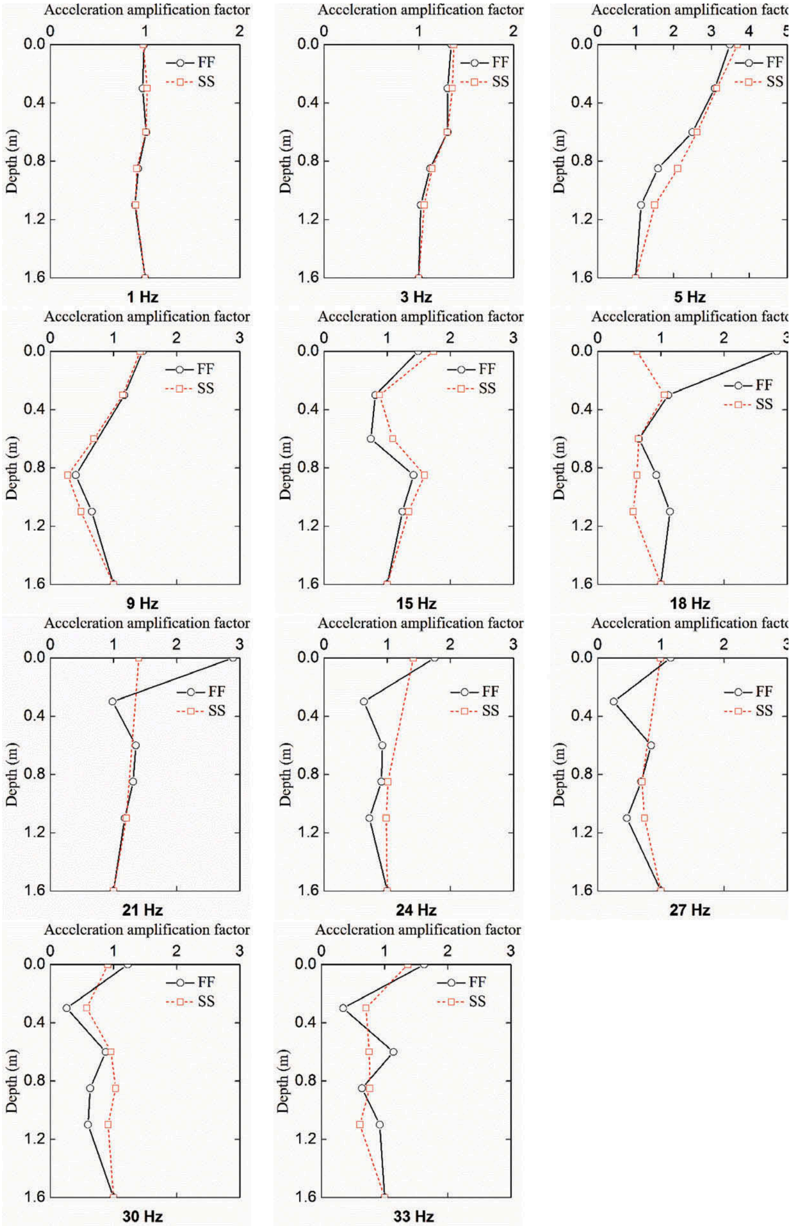

Figure 6. The comparison of acceleration response along the depth of soil.

than 15 Hz, the peak accelerations in different surface distances were almost the same. The minor differences at different points may be due to the fact that on the ground surface both the artificial soil and the accelerometers lack constraints. In shaking table test, measures are needed to avoid this kind of deviation. In addition, vertical boundary of the model container might also be an influence factor.

Two spectral peaks can be seen in Figure 7a: the first and second spectral peaks occurred at 5 Hz and 21 Hz, respectively, which were near the first and second natural frequencies of the ground layer, respectively. In the numerical study by Besharat et al. (2014), there were two typical characteristics for free-field model: first, the peak accelerations did not change significantly in middle of model and near side boundaries; second, the peak amplification was observed

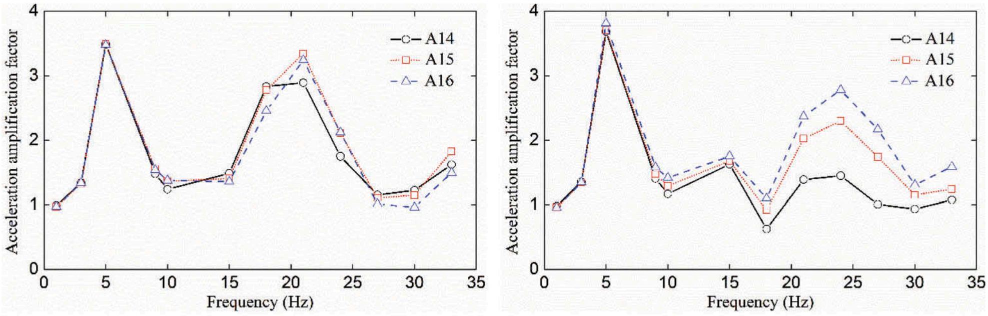

(a) Free-field model (b) Soil-station model

Figure 7. Acceleration amplification frequency spectra at different positions on ground surface.

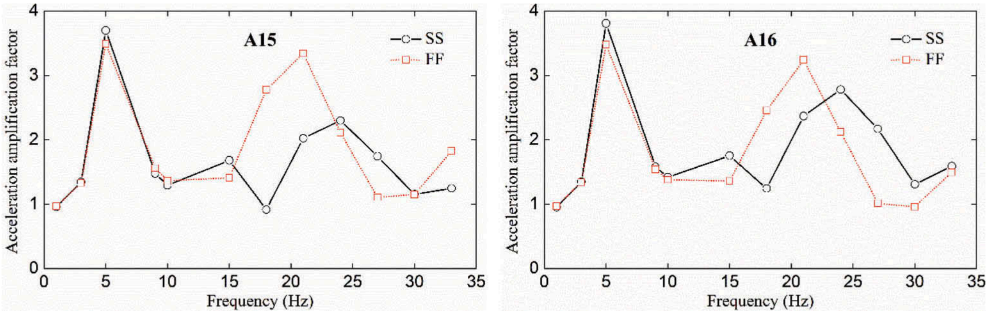

Figure 8. Comparisons of acceleration amplification frequency spectra for two models.

around 2.5 Hz in the range 0.5-7 Hz. The reason why there was no second spectral peak was that the authors only focused on the frequencies lower than 7 Hz, which were lower than the second natural frequency. For this study, tests were designed to include larger frequencies to evaluate their influence on the ground and structure. Overall, the two studies resulted to be consistent with each other for the frequencies near the first natural frequency of ground layer.

From Figure 7b it can be concluded that for soil-station model, as the distance from the sidewall increased, the acceleration amplification factors would increase towards those measured in free-field conditions (Figure 7a), but the influence was extremely frequency dependent. When the frequencies of input motion were lower than 15 Hz, the peak accelerations in different surface distances had very few discrepancies. The discrepancies became apparent when the frequencies were larger than 15 Hz. Althugh the first natural frequencies of the ground layer is not to be affected by the presence of the station, the second one increases to about 24 Hz compared to free-field.

Figure 8 compares acceleration amplification frequency spectra between free-field model and soil-station model at two points of A15 and A16, respectively. As illustrated in Figure 8, the existing of station structure had a much more significant effect on the surface ground accelerations for the frequencies larger than 15 Hz than those lower than 15 Hz. In comparison with the free-field model, the existing of atrium-style subway station tended to change the seismic site responses at high frequencies such as those near the second natural frequency of ground in this study. The affected areas were greater than 1.25 times the width of the structure in this study. To determine the exact affected area, conducting numerical analyses which is based on the test model is extremely necessary and this work is currently on-going.

4 CONCLUSIONS

1g shaking table tests were carried out to study the effect of an atrium-style subway station on the seismic ground responses both at the ground surface and along the depth of ground.

The test model was verified by comparing the results of free-field test to the analytical solutions. A comparison of the seismic ground responses between the free-field model and soil-structure model was conducted after the initial verification process. The shaking table tests have proven that: (i) the underground subway station did not affect free-field responses when the wavelength of incident wave were greater than 8 times the height of structure; (ii) the influence of distance from the station sidewall on surface ground acceleration responses was extremely frequency dependent; the existing of atrium-style subway station tended to change the surface ground acceleration responses at high frequencies such as those near the second natural frequency of ground in this study; (iii) the aforementioned affected areas were greater than 1.25 times the width of the structure in this study and the exact affected area is still to be determined by conducting additional numerical analyses.

ACKNOWLEDGMENTS

The research is mainly supported by National Key Research and Development Plan, China (2017YFC1500700) and State Key Laboratory of Disaster Reduction in Civil Engineering, the Ministry of Science and Technology of China (SLDRCE15-02).

REFERENCES

Alielahi, H., Kamalian, M., Adampira, M. 2015. Seismic ground amplification by unlined tunnels subjected to vertically propagating SV and P waves using BEM, *Soil Dynamics and Earthquake Engineering* 71(2015): 63-79.

Besharat, V., Davoodi, M., Jafari, M.K. 2014. Variations in ground surface responses under different seismic input motions due the presence of a tunnel, *Arabian Journal for Science and Engineering* (2014) 39: 6927-6941.

Assimaki, D., Kausel, E., Gazetas, G. 2005. Wave propagation and soil–structure interaction on a cliff crest during the 1999 Athens earthquake, *Soil Dynamics and Earthquake Engineering* 25(2005): 513-527.

Baziar, M.H., Moghadam, M.R., Kim, D.S., Choo, Y.W. 2014. Effect of underground tunnel on the ground surface acceleration, *Tunnelling and Underground Space Technology* 44 (2014): 10–22.

Tsinidis, G., Heron, C., Pitilakis, K., Madabhushi, G. 2014. Physical modeling for the evaluation of the seismic behavior of square tunnels, *Geotechnical, Geological and Earthquake Engineering*. Switzerland: Springer.

Moghadam, M.R., Baziar, M.H. 2016. Seismic ground motion amplification pattern induced by a subway tunnel: Shaking table testing and numerical simulation, *Soil Dynamics and Earthquake Engineering* 83(2016): 81-97.

Guan, Z., Gong, Z., Luo, Z., Chen, R., He, C. 2016. Seismic property of a large section tunnel based on shaking table model tests, *Rock and Soil Mechanics* 37 (9): 2553-2560.

Wang, G., Yuan, M., Miao, Y., Wu, J., Wang, Y. 2018. Experimental study on seismic response of underground tunnel-soil-surface structure interaction system, *Tunnelling and Underground Space Technology* 76 (2018): 145–159.

Guo, J. 2013. The dynamic deformation analysis of underground structures and its influence on seismic response of adjacent surface buildings, Ph.D Thesis, Dalian University of Technology, Dalian.

Hashash, Y., Dashti, S., Musgrove, M., Gillis, K., Walker, M., Ellison, K., Basarah, Y. 2018. Influence of tall buildings on seismic response of shallow underground structures, *Journal of Geotechnical and Geoenvironmental Engineering* 144(12): 04018097

DGJ08-37-2012. Code for investigation of geotechnical engineering.

Bao, Z., Yuan, Y., Yu, H.T. 2017. Multi-scale physical model of shield tunnels applied in shaking table test, Soil Dyn. Earthquake Eng. 100(2017),465-479.

Zhang, Z.M., Yuan, Y., Bilotta, E., Yu, H.T., Zhao, H.L. 2019. Design of shaking table tests on atrium-style subway station models under seismic excitation, *World Tunnel Congress,Naples*, *3-9 May 2019*.

Kramer, S.L., 1996. *Geotechnical Earthquake Engineering*. New Jersey: Prentice Hall.

Blackwell, C., Palazotto, A., George, T.J., Cross, C.J. The evaluation of the damping characteristics of a hard coating on titanium, *Shock and Vibration* 14(2007): 37-51.

Jiang, L., Yao, L., Wu, W., Xu, G. 2010. Transfer function analysis of earthquake simulation shaking table model test of side slopes, *Rock and Soil Mechanics* 31 (5): 1368-1374.